

# Application of Proper Orthogonal Decomposition (POD) to the analysis of velocity fields in turbulent impinging jet flow

A.V.Bilsky, P.R.Kaipov, D.M.Markovich, M.P.Tokarev

**Abstract** The POD has been applied to the ensembles of 2-D velocity fields obtained by means of Particle Image Velocimetry technique (PIV) for the case of turbulent axisymmetric impinging jets. The increase of spatial resolution of PIV measuring system was attained due to separation of investigated area into several zones. POD method allows to perform the statistical analysis of turbulent fields without attraction of additional assumptions usually used for decomposition of the flow characteristics into mean, pulsation and other (for instance, coherent) components. By analysis of POD eigenvalues that are proportional to the average kinetic energy of turbulent pulsations, the energy-favorable configurations were found and used in the reconstruction of velocity field on the basis of several first eigenmodes. The POD spectra have been compared for different Reynolds numbers of impinging jet flow and for two distinguished cases – with and without presence of external flow forcing.

**Keywords:** turbulent axisymmetric impinging jet, Proper Orthogonal Decomposition (POD), coherent structures, Particle Image Velocimetry (PIV).

## 1

### Introduction

The most widespread approach to analyze the turbulent flow characteristics is the decomposition of a signal into mean and fluctuation parts (Reynolds decomposition). Also the different kinds of triple decomposition are often used to distinguish the coherent part of the signal (e.g. conditional averaging decomposes fluctuations into regular and stochastic parts). Both approaches have certain restrictions: the Reynolds decomposition does not allow to identify turbulent scales while conditional averaging demands some a priori knowledge of the flow structure. One of alternative approaches to analyze turbulent flow structure is the Proper Orthogonal Decomposition (POD). POD allows to study turbulent flows without using any additional assumptions.

POD technique was introduced by Lumley (1967) in order to recognize the coherent structures in turbulent flows. By using POD, one can provide the modal decomposition of an ensemble of functions – fields of experimental database. Such a decomposition has one of the most important features: it is optimal from the energetic point of view, i.e. the finite series of the modes and coefficients can describe the energetic contents of the flow including the most powerful coherent structures.

In the near field of axisymmetric shear layers and jets the coherent structures play dominant role in the transition to the developed turbulence and mixing processes. In the early work by Leib et al. (1984) the application of POD to the analysis of undisturbed axisymmetric shear layer has demonstrated the possibility to describe evolution of the flow in terms of POD analysis. Glauser & George (1987) studied near field of the jet shear layer. They have shown that the first POD mode contains about 40 % of total flow energy and only a few modes are needed to describe the flow from energy point of view. Latter publications by Ukeiley & Seiner (1998), Ukeiley et al. (1999) were related to the study of supersonic jets by using contact techniques (rake of probes). Considerable changes of the eigenmodes were observed downstream of the jet flow. The POD was utilized for investigation of the turbulent plane jet flow and mixing layer in the study of Gordeyev & Thomas (2000), where main emphasis was focused on the similarity region of a turbulent planar jet, while Delville et al. (1999) reported a thorough examination of the POD modes in a plane mixing layer. The most comprehensive study of the axisymmetric jet flow with the use of POD applied to the HWA (hot wire anemometer) velocity fields of the near and far jet regions was performed by Jung et al. (2004).

---

A.V.Bilsky, P.R.Kaipov, D.M.Markovich, M.P.Tokarev

Correspondence to:

D.M.Markovich, Institute of Thermophysics SB RAS, Lavrentyev ave., 1, 630090, Novosibirsk, Russia, E-mail: dmark@itp.nsc.ru

Application of POD allowed to observe ‘volcano-type’ eruptions at 2 to 3 diameters downstream as well as ‘propeller-like’ pattern where the number of blades diminishes downstreams. For the far field of a jet the evolution of the most energetic features was investigated, high degree of similarity for POD eigenspectra was found. The modal content of the eigenspectra was also analyzed there.

Graftieaux et al. (2001) while studying turbulent swirling flows in a steady geometry applied the POD to the ensemble of instantaneous velocity fields measured by Particle Image Velocimetry. Velocity field was presented as a superposition of small- and large-scale turbulent pulsations. It was shown that the first eigenmode of decomposition contains up to 60 % of the total turbulent kinetic energy of the flow. Kim et al. (2003) investigated the global structure of the flow around a three-dimensional rectangular prism on the basis of PIV measurements. Bernero & Fiedler (2000) applied POD to the PIV measurements of the jet in counterflow with the same velocity to obtain the characteristic jet column frequency. The array of impinging circular jets was investigated using PIV and POD analysis of obtained velocity fields (Geers et al., 2005). The clear identification of the near-wall dominating vortical structure is found to be possible by POD.

PIV measurements of the impinging jet flow together with conditional sampling approach made it possible to get instantaneous flow pattern at a fixed phase of coherent structure and to analyze phase-by-phase dynamics of the coherent structures and other scales (Alekseenko et al., 2004). Main disadvantage of the conditional sampling approach is that one needs to impose periodical external disturbances in order to force the coherent structures to be strictly periodical. These disturbances affect the flow in a way that has to be analyzed further. Applying POD to the statistical ensemble of velocity fields allows to evaluate the effect of external forcing on energy structure of a jet and to find the energy-optimal configurations of the flow. Inverse POD with numerable number of eigenvectors gives accurate or approximate reconstructions of initial flow pattern.

The present work is devoted to the POD analysis of the ensemble of PIV-measured velocity fields of impinging jets under both unforced and low-amplitude forced conditions. Two essentially different Reynolds numbers of the flow are considered –  $Re = 7600$  (transitional jet flow) and  $Re = 34100$  (developed turbulent jet flow).

## 2

### Decomposition method

The POD basic idea consists in representation of a turbulent field of velocity as a finite series of products of spatial orthonormal functions (the basis) with temporal coefficients:

$$u(x, t_i) = \sum_{n=1}^N a_n(t_i) \cdot \varphi_n(x); \quad \langle \varphi_n(x), \varphi_m(x) \rangle_x = \delta_{mn} . \quad (1)$$

Mathematical interpretation of this decomposition consists in representation of each term of statistical ensemble  $u(x, t_i)$  as a point in  $N$ -dimensional space (generally infinite-dimensional) with the certain procedure of scalar product, and functions  $\varphi_n(x)$  being the orthonormal basis in this space. Thus coefficients  $a_n(t_i)$  are the projections of a velocity vector onto basis POD vectors.

To determine the optimal orthonormal basis (1) it is necessary to find a set of vectors  $\varphi_n(x)$  providing a maximum for the functional (Sirovich, 1987):

$$\frac{\langle |(u(x, t_k), \varphi(x))|^2 \rangle_k}{(\varphi(x), \varphi(x))} = \lambda \rightarrow \max , \quad (2)$$

Solution of the variational problem (2) results in the homogeneous Fredholm integral equation of the second kind:

$$\int K(x, x') \varphi(x') dx' = \lambda \varphi(x), \quad (3)$$

where either a cross-correlation function (at  $N = \infty$ ) or a symmetric tensor of two points  $x$  and  $x'$  (at  $N \rightarrow \infty$ ) is used as a kernel of the integral operator:

$$K(x, x') = \frac{1}{N} \sum_{k=1}^N u(x, t_k) u(x', t_k). \quad (4)$$

It is possible to represent the eigenvectors  $\varphi_n(x)$  of correlation matrix as the following sum (the snapshot method, Sirovich (1987)):

$$\varphi_n(x) = \sum_{k=1}^N A_k^n \cdot u(x, t_k). \quad (5)$$

The snapshot method is widely used to obtain the coefficients in decomposition (1) when the statistical ensembles of velocity fields measured by PIV are analyzed.

Substitution of (5) into equation (3) leads to the following equation:

$$\frac{1}{N} \sum_{m=1}^N \left[ \int u(x, t_n) \cdot u(x, t_m) dx \right] A_m^i = \lambda_i A_n^i. \quad (6)$$

The solution of eigenvectors/eigenvalues problem (6) allows to determine  $N$  eigenvectors  $A_i$  and corresponding eigenvalues  $\lambda_i$  for calculation of the basis vectors  $\varphi_n(x)$ . By virtue of the matrix symmetry the eigenvalues have a property:  $\lambda_i > 0$  (for any  $i$ ). Additionally it is possible to demand:  $\lambda_{i-1} \geq \lambda_i > 0$  ( $i = 2, \dots, N$ ). In the present work the solution of problem (6) was done, accounting for the matrix symmetry, by QR-algorithm of reducing the matrix to a three-diagonal form.

The analysis of coefficients and basis vectors of POD allows to define the following properties:

1) temporal coefficients of POD are not statistically correlated quantities:

$$\langle a_n(t) a_m(t) \rangle_t = \lambda_m \delta_{mn} \quad (7)$$

2) the eigenvalues  $\lambda_i$  of correlation matrix  $K(x, x')$  are proportional to average kinetic energy of turbulent pulsations for corresponding POD basis. The sum of all eigenvalues specifies the full average kinetic energy of turbulence. These properties follow from the equation:

$$\langle u(x, t) u(x, t) \rangle_t = \int K(x, x) dx = \sum_{n=1}^N \left\langle \left| (u(x, t), \varphi_n(x)) \right|^2 \right\rangle_t = \sum_{n=1}^N \lambda_n. \quad (8)$$

The description of ensemble of velocity fields in terms of POD leads to determination of the finite set of configurations (velocity fields) characterizing the investigated hydrodynamic object. The eigenvalue number  $\lambda$  proportional to the average kinetic energy of turbulence, is associated with each configuration. The first configuration (POD mode) corresponding to the largest  $\lambda$  contains the most part of mean kinetic energy. The decomposition performed in the present work for instantaneous velocity fields of impinging jets has shown that the first POD mode corresponds to the mean flow (to an accuracy of a constant). For the fluctuation velocity fields analysis (with subtraction of the mean flow) the shift of eigenvectors and eigenvalues has been observed (the second POD mode for ensemble of instantaneous velocity fields corresponds to the first POD mode of ensemble of pulsations of velocity fields).

### 3 Experimental setup

In the present work the submerged axisymmetric impinging water jet oriented normally to the impingement plate has been studied (Figure 1). Nozzle-to-plate distance was equal to  $H = 45$  mm and the nozzle diameter was  $d = 15$  mm. The coordinate system origin was located at the jet stagnation point. Reynolds numbers based on the nozzle exit maximum velocity and the nozzle diameter were  $Re=7600$  and  $Re=34100$ . During measurements the water temperature and the flow rate were kept stabilized.

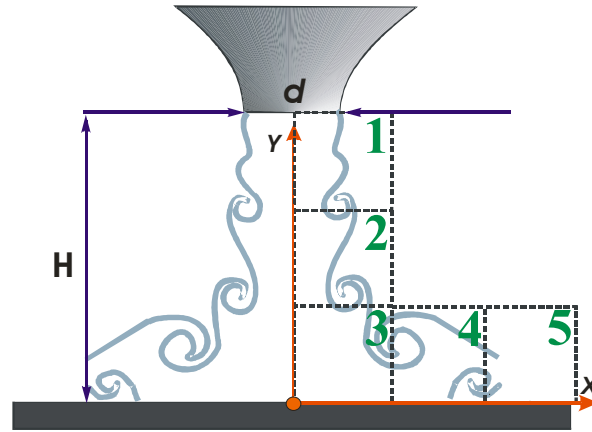


**Figure 1** Axisymmetric impinging jet. Whole velocity field is divided into five equal elementary zones.  
 $D = 15 \text{ mm}$ ,  $H/d = 3$ .

To measure velocity fields the 2-D PIV system was used. The PIV system consisted of double cavity Nd:YAG laser and Dantec HiSense cross-correlation camera which registered the light scattered by particles. To obtain the instantaneous velocity fields from images the “Actual Flow” software which is part of “PIVIT” measurement system has been used. Iterative cross-correlation approach with window deformation and 50% overlapping was chosen to calculate velocity fields with reduced bias error (see Scarano (2002) for details). Initial and final interrogation window sizes were 64x64 and 32x32 pixels, correspondingly. In order to reduce the number of spurious vectors (outliers) in the near-nozzle and near-plate regions the No-DC filter was applied. The statistical filtering procedure (Heinz et al., 2004) was also employed during processing.

To implement the conditional sampling approach the external forcing with frequency  $f$  corresponding to the frequency of the jet most sensitivity (and the amplitude significantly smaller than the jet turbulent intensity level) was applied. Strouhal number based on the nozzle diameter and the jet maximum velocity was equal to  $Sh=f*d/U=0.5$ . The ensembles of velocity fields were measured for unforced and forced jet conditions and also for some chosen phase of flow assuming the coherent structures to be “frozen”.

In order to increase the spatial resolution of the measurements the whole jet region has been divided into five sub-areas (15x15mm) as shown in Figure 1. This allowed us to increase the spatial resolution up to 0.26 mm per vector. For each of the five areas 1500 instantaneous velocity fields were measured for both cases – forced ( $Sh = 0.5$ ) and unforced ( $Sh = 0$ ). To perform triple decomposition (conditional sampling) in the case of external forcing 1000 instantaneous velocity fields were measured for each phase of the coherent structure’s propagation period. Overall number of phases was equal to 20.

#### 4 Results

Let’s first consider the conditional sampling approach for impinging jet flow analysis. Such a flow under the conditions of periodic forcing with the frequencies within the range of the jet most sensitivity ( $Sh = 0.4 \div 0.7$ ) is periodic in the near field of the jet with well pronounced large-scale vortex structures (Alekseenko et al., 1997). This fact allowed us to perform the triple decomposition of measured velocity in order to separate the coherent and broad-band components of physical quantities. According to the common approach the triple decomposition for instantaneous value of generalized variable  $a$  is (Hussain and Reynolds, 1972):

$$a(\vec{x}, t) = \bar{a}(\vec{x}) + \tilde{a}(\vec{x}, t) + a'(\vec{x}, t), \quad (9)$$

where first, second and third terms in the R.H.S. of equation (9) are correspondingly the average, coherent (periodic) and stochastic components of pulsations. In the present work the velocity vector has been considered as a partial case of  $a$ . Conditional sampling was provided by synchronisation of excitant signal with laser pulses and setting the corresponding phase delay. Both centralized and non-centralized (relative to time-averaged values) characteristics were calculated.

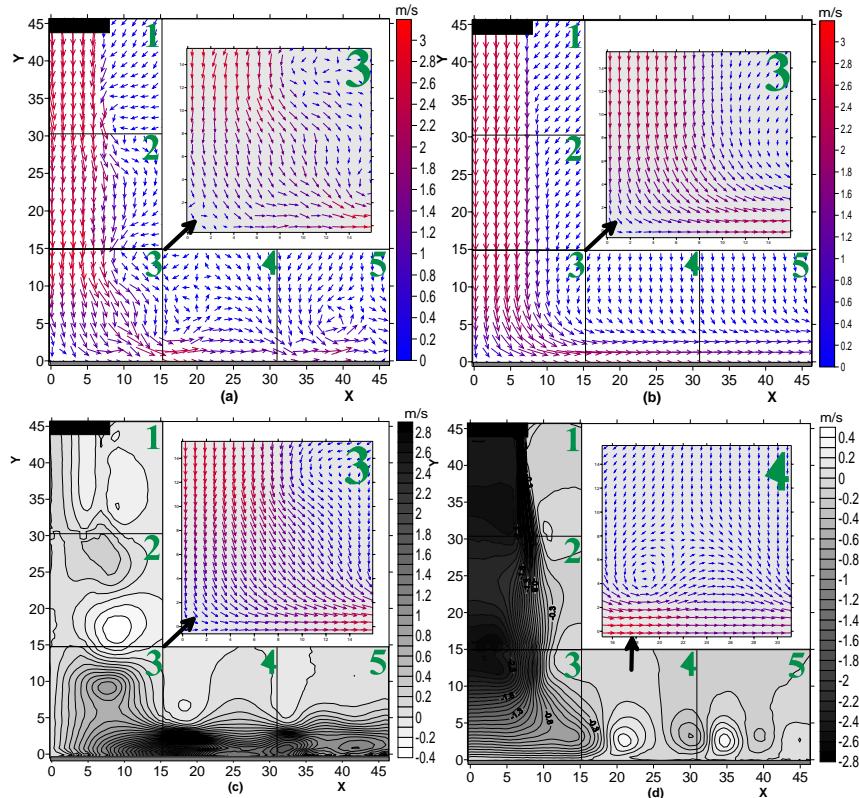


**Figure 2** Hydrodynamic characteristics of the impinging jets at  $Re = 34100$ : (a) instantaneous velocity field (unforced case,  $Sh=0$ ), (b) averaged velocity field (unforced case,  $Sh=0$ ), (c,d)  $U$  and  $V$  component of velocity in fixed phase of coherent structures (forced case,  $Sh=0.5$ ).

Velocity fields shown in Figure 2 were measured for impinging jet under unforced (a,b) and forced (c,d) conditions for each of the five selected zones. Instantaneous, whole-averaged and conditionally averaged velocity distributions are presented. By means of conditional sampling technique the coherent component of turbulent pulsations is extracted. Figure 2 (c, d) presents the phase-averaged distributions of velocity components. The “frozen structure” of the flow averaged only over the stochastic part of turbulent pulsations can be seen. One can clearly observe the periodic spatial flow structure caused by large vortices. The examples of detailed distributions for 3<sup>rd</sup> and 4<sup>th</sup> sub-areas are presented in the squares (for better view every third vector is shown). One can observe localized vortex, averaged in the chosen phase, which propagates downstream in the jet mixing layer.

For the unforced flow conditions it is impossible to perform similar analysis, however the developed large-scale structures exist in such a flow also, but their propagation is quasi-periodical at the best. Besides, even for forced flow conditions, the conditional sampling technique have to enforce some restrictions because in this case too the condition of ideal periodicity is not exactly valid and some information about smaller structures is often lost.

POD is one of alternative methods allowing to perform the flow analysis without any additional conditions. In this work POD has been applied to ensembles of instantaneous velocity fields and fields of velocity pulsations to each of the five elementary zones shown in Figure 1. Figure 3 demonstrates dependencies of POD eigenvalues at  $Re = 34100$  versus relative eigenmode numbers (POD spectra). In order for better comparison of spectra for different zones and experimental conditions the results are presented in the form of normalized cumulative sum which represents the ratio between the energy contained in the  $i$ -th mode and the global energy contained within the flow (the value of  $j/N$  is put at abscissa axis):

$$\lambda'_j = \frac{\sum_1^j \lambda_i}{\sum_1^N \lambda_i}. \quad (10)$$

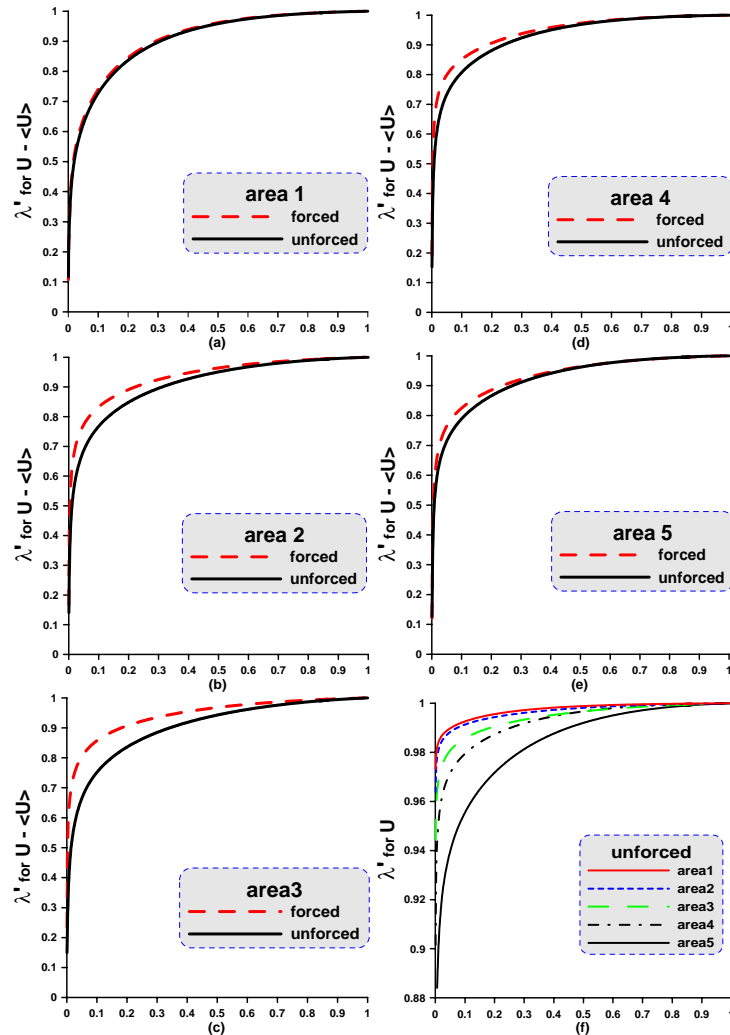


**Figure 3** The evolution of normalized cumulated eigenvalues versus normalized modes for fluctuation velocity fields. Results for forced and unforced impinging jets and for all measurement areas are presented. (a) – area 1, (b) – 2, (c) – 3, (d) – 4, (e) – 5. (f) – comparison of spectra for all areas (unforced impinging jet).

Figure 3 (a-e) presents the comparison of POD spectra for the forced and unforced cases for different areas of the impinging jet flow. It is clearly seen from the Figure that in the 1<sup>st</sup> and 5<sup>th</sup> zones where the coherent structures are non-pronounced “yet” and “already” correspondingly, the flow structure from the “POD point of view” is very similar for forced and unforced cases. At the same time for zones 2-4, where coherent structures are more powerful at forced conditions, the difference between POD spectra is more pronounced: for the forced case they change more abruptly at smaller  $j/N$ . It means that larger part of turbulent energy is contained in smaller number of POD modes and manifests the role of energy redistribution in the flow with developed large-scale structures.

The eigenvalues are calculated for instantaneous velocity field (Fig. 3, f) and fluctuation fields (Figs. 3, a-e). First eigenvalue of POD of ensemble of instantaneous velocity fields is proportional to kinetic energy of the mean flow and contains up to 80 % of the total amount of kinetic energy. In Figure 3, f, the comparison of the POD spectra is shown for different measurement zones for unforced case. The spectra of instantaneous velocity fields are presented. The role of mean flow is demonstrated here: if for the 1<sup>st</sup> zone almost all the kinetic energy is contained in the 1<sup>st</sup> POD mode, on the contrary, for the far field of flow (developed wall jet – 5<sup>th</sup> zone) the behavior of the spectrum is much more gradual and energetic structure of the flow can be described by larger number of POD modes.

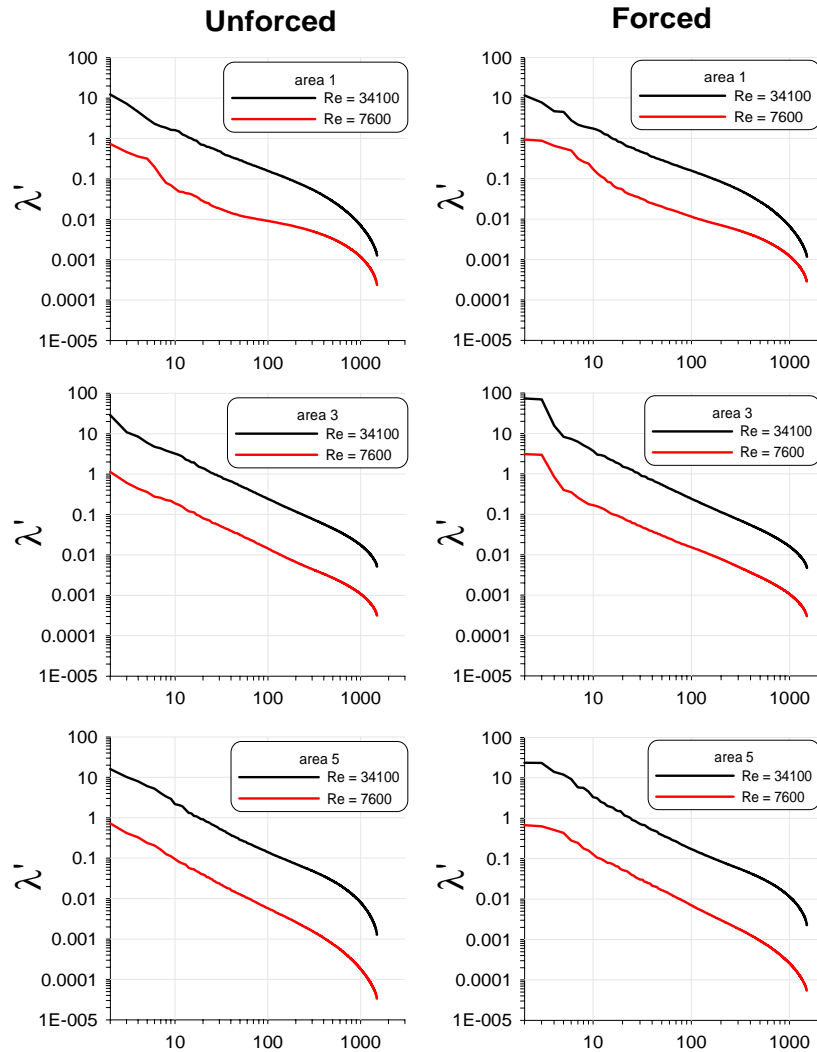


**Figure 4** POD eigenvalue spectra for the 1<sup>st</sup>, 3<sup>rd</sup> and 5<sup>th</sup> measurement zones. Comparative representation for  $Re = 7600$  and  $34100$  and forced/unforced conditions.

The spectra presented in Figure 4 show the eigenvalues of the POD for two different Reynolds numbers  $Re = 7400$  and  $34100$  both for forced ( $Sh = 0.5$ ) and unforced jet ( $Sh = 0$ ). The ensembles of fluctuation fields are processed in this case and three elementary flow zones are compared (1<sup>st</sup>, 3<sup>rd</sup> and 5<sup>th</sup>, see Figure 1). The eigenvalues are plotted against the mode number in logarithmic coordinates. The behavior of spectra is very similar for both Reynolds number as well as for forced and unforced flow conditions – monotonic decrease of energy towards the large values of mode number takes place. Obviously the overall level of turbulent kinetic energy is essentially larger for large Reynolds number,  $Re = 34100$ , so the corresponding curves lie somewhat higher. More clear pattern can be seen from Figure 5 where normalized cumulated eigenvalues are plotted versus normalized modes for 1<sup>st</sup>, 3<sup>rd</sup> and 5<sup>th</sup> measurement zones. Such representation, as it was noted above, allows to estimate the necessary minimum of eigenmodes sufficient for complete enough energetic description of the flow. Analysis has shown that for the far field of a jet, starting from the 3<sup>rd</sup> zone, the normalized spectra for both Reynolds numbers are very close to each other both for forced and unforced cases. Moreover, low- $Re$  curves are situated somewhat upper in the far field of the jet (5<sup>th</sup> zone) than for higher Reynolds number. Such a difference is also observed during comparison of forced and unforced cases for  $Re=34100$  (see Figure 3). The forced jet flow as well as low- $Re$  jet flow, due to energy concentration in the large-scale range, has obviously some narrower turbulent spectrum in comparison with high- $Re$  unforced flow where energy spectrum should be wider. As for the jet near-field (zone 1), turbulence is not developed at low  $Re$ , so correct comparison of spectra is rather difficult.

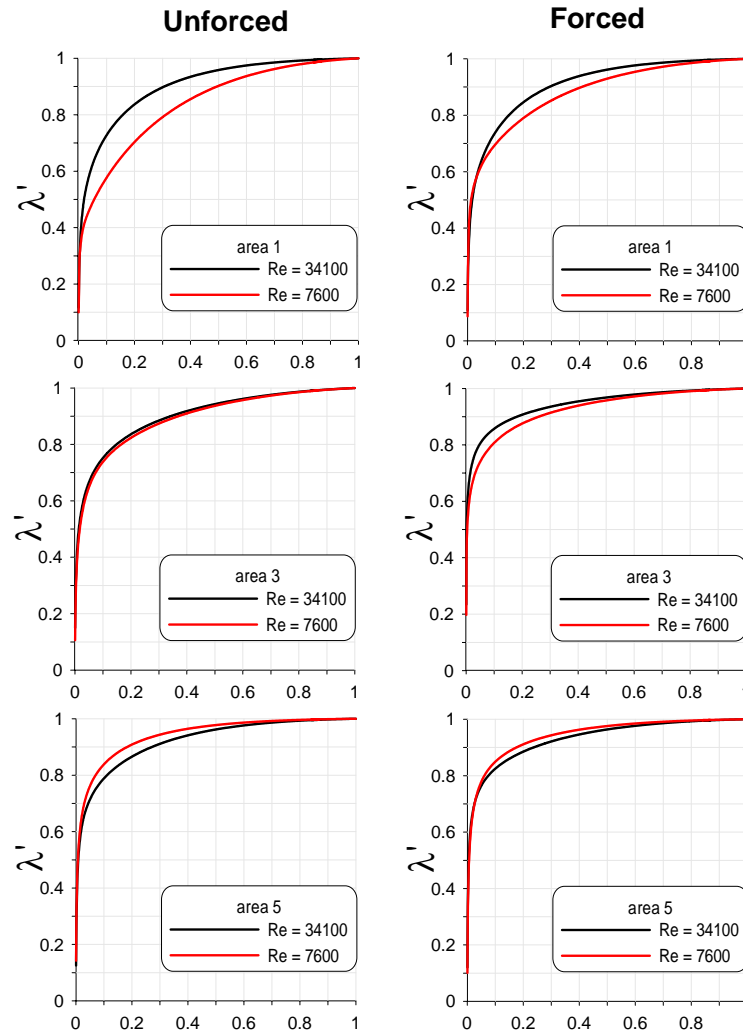


**Figure 5** Evolution of normalized cumulated eigenvalues versus normalized modes for the 1<sup>st</sup>, 3<sup>rd</sup> and 5<sup>th</sup> measurement zones. Comparative representation for  $Re = 7600$  and  $34100$  and forced/unforced conditions.

Obtained results are in some contradiction with the conclusion of the paper of Patte-Rouland et al. (2001), where the evolution of POD eigenvalues for an annular jet with two different Reynolds numbers is analyzed. Authors stated that  $\lambda'_j$  increases with increasing exit nozzle velocity, so the number of modes with low energy ratio rises. The conclusion was done that this is in agreement with turbulence theory: the number of small structures increases with the Reynolds number. Probably this statement is valid for Reynolds numbers considered by Patte-Rouland et al. – 7680 and 2048, because latter one is rather low and obviously turbulence is not developed.

Following the approach of Geers et al. (2005) let's analyze the energy distribution over the first few modes. The summarizing Table 1 presents the summed values for the energy contained in the groups of ten modes. For first ten modes the more detailed layout is also presented. The mode 0 corresponding to average velocity field is not taken into account, thus only the energy of fluctuations is analyzed. It can be seen from the Table that first 10 modes contain from 33 % to 62 % of total fluctuation energy depending on the flow regime, Reynolds number and zone of testing. At the same time Geers et al. (2005) stated for multiple impinging jet experiments ( $H/d = 4$ , unforced conditions,  $Re = 18000 \div 20000$ ) that approximately one-third of the total energy is contained in the first 20 modes. If we consider mostly close conditions from present experiments, for example, the unforced case and  $Re = 34100$ , it can be concluded that the energy content value averaged over 5 different zones for the first 20 modes is not smaller than 50%. At the same time for zones containing the developed large-scale vortex structures (zones 2-4) up to 50% of energy can be contained in the first 3 modes in some cases (see Table 1).



Table 1. Energy contents for POD eigenmodes.

Regime		Zone/Mode	1-3	4-6	7-10	1-10	11-20	21-30	31-40	41-50
Re = 7600	unforced	Zone 1	21,1	8,6	3,5	33,2	5,0	2,9	2,1	1,8
		Zone 2	25,5	10,2	7,3	43,0	9,7	4,9	3,4	2,5
		Zone 3	20,3	8,3	7,5	36,1	10,0	5,8	4,1	3,2
		Zone 4	35,9	9,3	6,2	51,4	7,6	4,5	3,2	2,5
		Zone 5	29,0	12,0	8,2	49,2	10,3	5,5	3,7	2,7
	forced	Zone 1	16,9	16,0	9,2	42,1	7,6	3,6	2,6	2,1
		Zone 2	32,6	6,0	5,4	44,0	8,3	4,8	3,4	2,6
		Zone 3	44,1	6,5	4,5	55,1	6,6	3,8	2,7	2,1
		Zone 4	43,0	10,0	7,5	60,5	7,9	4,0	2,7	2,0
		Zone 5	27,3	14,4	8,6	50,3	10,6	5,6	3,7	2,8
Re = 34100	unforced	Zone 1	22,9	7,1	6,2	36,2	8,7	5,2	3,7	3,0
		Zone 2	26,2	10,1	7,1	43,4	9,1	5,0	3,5	2,7
		Zone 3	25,0	7,8	7,0	39,8	9,6	5,3	3,7	2,9
		Zone 4	30,3	10,9	7,4	48,6	9,3	5,0	3,4	2,5
		Zone 5	26,6	11,9	8,3	46,8	9,3	5,0	3,3	2,5
	forced	Zone 1	22,2	8,8	6,6	37,6	9,2	5,1	3,7	2,9
		Zone 2	40,5	9,2	6,8	56,5	8,0	4,2	2,8	2,1
		Zone 3	50,5	6,9	5,2	62,6	6,6	3,7	2,5	1,9
		Zone 4	42,7	12,2	6,7	61,6	7,1	3,8	2,4	1,8
		Zone 5	31,2	13,9	8,6	53,7	9,1	4,5	3,0	2,2

In Figure 6 the first two basis vectors (modes) of POD are presented for each of the five measurement zones. The analysis of vector patterns shows that, to a factor of normalization, the first POD mode corresponds to ensemble averaged velocity field. External periodic forcing of the impinging jet flow essentially affects all basis vectors of POD decomposition. Each mode contains the vortex formations alternating in consecutive POD modes. The structure and configuration of POD basis essentially differs from the coherent component of turbulent pulsations obtained by means of conditional averaging technique (see Figure 2, c, d).

Each instantaneous velocity field  $u(x, t_i)$  from the ensemble of  $N$  measured snapshots can be expanded into series of  $N$  members. Taking into account all POD basis functions (modes) and temporal coefficients  $a_n(t_i)$ , it is possible to perform an inverse reconstruction of any snapshot from the ensemble. During this operation one can use a finite number of first POD modes ( $K < N$ ) containing the most part of turbulent kinetic energy (POD filtering):

$$u^K(x, t_i) = \sum_{n=1}^K a_n(t_i) \cdot \varphi_n(x) \quad (11)$$

Figure 7 (a) shows one snapshot from the ensemble of original instantaneous fields of velocity pulsations for the 2<sup>nd</sup> measurement area of impinging jet. POD filtering has been also performed with different number of modes taken as a basis. In Figures 7, b-f, the reconstructed snapshots are shown versus parameter  $K$ . The relative error of restoration of an initial velocity field at  $K=N=1500$  does not exceed 3 %, at  $K = 1000 - 10$  %. For small values of  $K$  (from 1 to 10) configurations of the restored snapshots do not differ substantially. In specified zones (2<sup>nd</sup> measurement area), where large-scale structures are rather developed, the low- $K$  restored snapshot also contains vortex structures, which however do not completely reflect the physical nature of the flow.

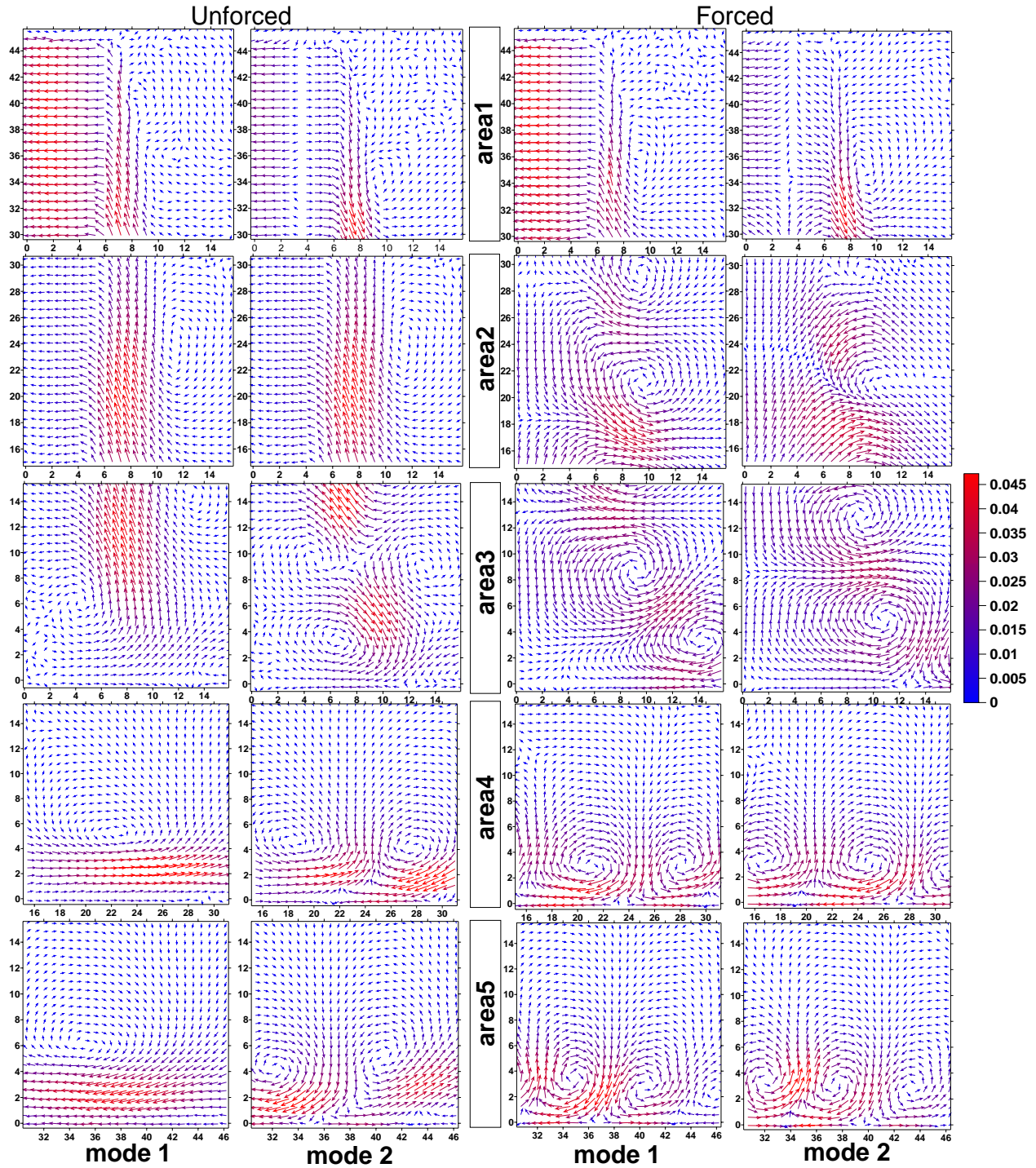
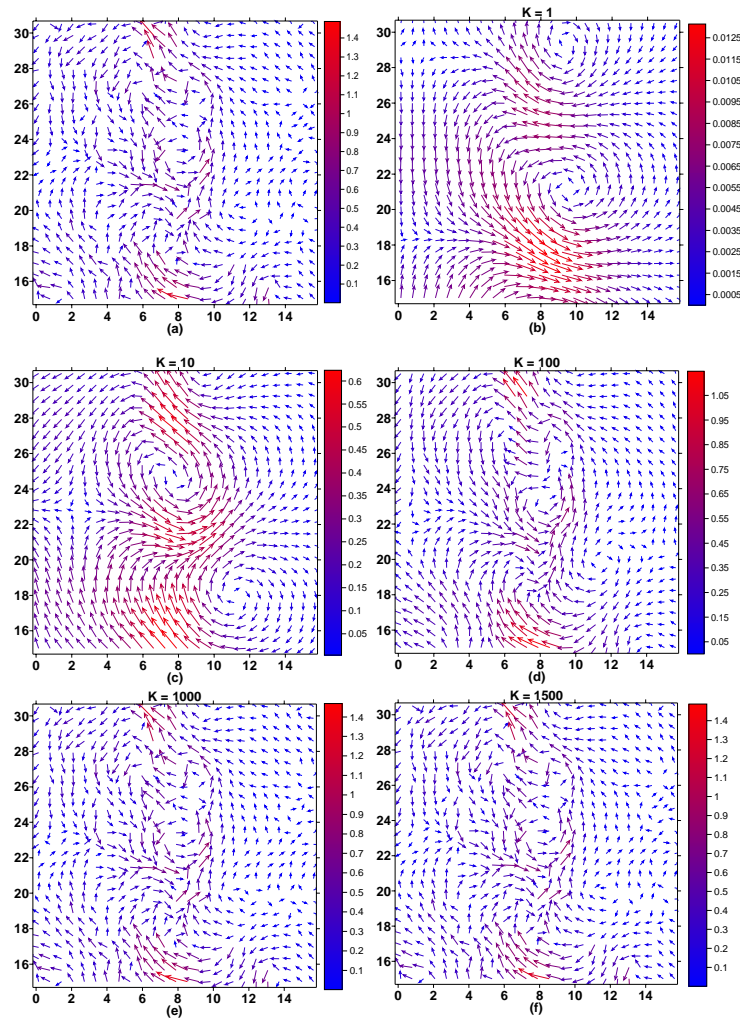


Figure 6 POD basis for velocity fluctuation of impinging jet.



**Figure 7.** Reconstructed snapshots  $u^K$  of the impinging jet velocity field. 2<sup>nd</sup> measurement area. (a) original snapshot, (b) reconstructed snapshot for  $K = 1$  (first POD mode), (c)  $K = 10$ , (d)  $K = 100$ , (e)  $K = 1000$ , (f)  $K = 1500$  (full reconstruction).

## 5 Conclusions

In this paper the turbulent structure of the impinging jet was studied using PIV measuring system. The whole measurement area was divided into small sub-areas which allowed to increase the spatial resolution up to 0.26 mm per vector. Proper Orthogonal Decomposition allowed us to perform analysis of the turbulent velocity pulsations without any special assumptions. By means of POD of velocity fields the most energy-optimal modes were found. It was shown that for impinging jet the most part of energy is contained in a few first eigenmodes. First eigenmode, which corresponds to an ensemble averaged flow contains up to 80% of the total energy. The number of eigenmodes that contain the essential part of kinetic energy decreases with increasing the distance from the jet origin. External periodic forcing of the flow which is needed to perform the conditional sampling affects eigenvectors and eigenvalues of POD strongly. Reconstruction of the initial velocity fields was performed using inverse decomposition. Reconstruction based on the complete set of eigenvectors gives the accuracy of about 3% compared to initial velocity field.

## 6 Acknowledgments

This work was supported by Russian Foundation for Basic Research, grant N 04-02-16907 and Russian Science Support Foundation.

## 7

**References**

- Alekseenko, S.V., Bilsky, A.V. & Markovich, D.M.** (2004) Application of the method of Particle Image Velocimetry for analyzing turbulent flows with a periodic component. *Instruments and Experimental Techn*, No. 5, pp. 145-153
- Alekseenko, S.V., Markovich, D.M. and Semenov, V.I.**, (1997) Effect of external disturbances on the impinging jet structure. *Proc. of the 4<sup>th</sup> World Conference on Experimental Heat Transfer, Fluid Mech. and Thermodynamics*, Brussels, June 2-6, vol. 3, pp. 1815-1822.
- Berkooz G, P Holmes, J L Lumley** (1993) The proper orthogonal decomposition in the analysis of turbulent flows, *Fluid Mech.*, 25. 539-575.
- Bernero S., H.E. Fiedler** (2000) Application of particle image velocimetry and proper orthogonal decomposition to the study of a jet in a counterflow – *Experiments in Fluids*, S247 – S281.
- Delville J., Ukeiley L., Cordier L., Bonnet J.-P., Glauser M. N.** (1999) Examination of large scale structures in a plane mixing layer. Part 1. *J. Fluid Mech.* 391, 91–122.
- Gamard S., Jung D., George W.K.** (2004) Downstream evolution of the most energetic modes in a turbulent axisymmetric jet at high Reynolds number. Part 2. The far-field region. *J. Fluid Mech.*, vol. 514, pp. 205–230.
- Geers L.F.G., M.J. Tummers, K. Hanjalic** (2005) Particle imaging velocimetry-based identification of coherent structures in normally impinging multiple jets. *Physics of Fluids*, V.17, N5, Article N055105, 13 pages.
- Glauser M.N., George W.K.** (1987) An orthogonal decomposition of the axisymmetric jet mixing layer utilizing cross-wire measurements, 6th Symposium on Turbulent Shear Flow, Toulouse, France.
- Gordeyev S**, (1999) Investigation of coherent structure in the similarity or the planar turbulent jet using POD and wavelet analysis. PhD Thesis.
- Gordeyev S., Thomas F.** (2000) Coherent structure in the turbulent planar jet. *J. Fluid Mech.* 414, 145–194.
- Graftieaux L, M Michard and N Grosjean** (2001) Combining PIV, POD and vortex identification algorithms for the study of unsteady turbulent swirling flows - *Meas. Sci, Technol.* 12 1422-1429.
- Heinz, O., Ilyushin, B., Markovich, D.** (2004) Application of a PDF based method for the experimental statistical processing of experimental data”. *Int. J. Heat and Fluid Flow*, Vol. 25, pp. 864-874.
- Hussain, A. K. F. M., and Reynolds, W. C.** (1972) The mechanics of an organized wave in turbulent shear flow. Part 2, experimental results, *J. of Fluid Mech.*, vol. 54, pp. 241-261.
- Jung D., Gamard S., George W.K.** (2004) Downstream evolution of the most energetic modes in a turbulent axisymmetric jet at high. Reynolds number. Part 1. The near-field region. *J. Fluid Mech.*, vol. 514, pp. 173–204.
- Kim K.C., H.S. Ji, Y.G. Kim** (2003) PIV/POD studies on dynamic structures in the flow around a rectangular prism – 5th International Symposium on Particle Image Velocimetry, Busan, Korea.
- Liberzon R. Gurka, G.Hetsroni** (2001) Vorticity characterization in a turbulent boundary layer using PIV and POD analysis, 4th International Symposium on Particle Image Velocimetry, Gottingen, Germany, 17-19.
- Leib S. J., Glauser M. N., George W. K.** (1984) An application of Lumley's orthogonal decomposition to the axisymmetric jet mixing layer. *Proc. 9th Rolla Symp.* University of Missouri, Rolla.
- Lumley J. L., Holmes P & Berkooz G** (1993) The proper orthogonal decomposition in the analysis of turbulent flows – *Ann. Rev. Fluid Mech.* V. 25, pp. 539-575.
- Lumley J. L.** (1967) The structure of inhomogeneous turbulent flows. In: *Atmospheric Turbulence and Radio Waves Propagation* (ed. A. M. Yaglom & V. I. Tartarsky), p. 166. Nauka, Moscow.
- Patte-Rouland B, G Lalizel, J Moreau and E Rouland** (2001) Flow analysis of an annular jet by particle image velocimetry and proper orthogonal decomposition – *Meas. Sci, Technol.* 12 1404-1412.
- Santa Cruz, D. Calluaud, J. Pecheux, L. David** (2001) The proper orthogonal decomposition from PIV measurements to compare flows, 4th International Symposium on Particle Image Velocimetry, Gottingen, Germany, 17-19.
- Scarano F.** (2002) Iterative image deformation methods in PIV. Review article. *Meas. Sci. Technol.*, 13, p. R1-R19
- Sirovich L** (1987) Turbulence and the Dynamics of Coherent Structure: I, II, III, *Quarterly Applied Mathematics*, 45, p. 561-571.
- Ukeiley L., Seiner J.** (1998) Examination of large scale structures in a transonic jet mixing layer. *Proc. ASME Fluids Engineering Conf. ASME FEDSM 98-5234.*
- Ukeiley L. S., Seiner J. M., Ponton M. K.** (1999) Azimuthal structure of an axisymmetric jet mixing layer. In *Proc. 3rd ASME/JSME Joint Fluids Engineering Conf. ASME FEDSM 99-7252.*